Available online at www.sciencedirect.com
ScienceDirect
Journal of the European Ceramic Society 31 (2011) 783–787
www.elsevier.com/locate/jeurceramsoc

Improvement of the magnetic properties of highly porous open-celled magnets

Ugur Topal [a,*], Halil I. Bakan [b]

[a] TUBİTAK, UME (National Metrology Institute), P.K. 54, Gebze 41470, Kocaeli, Turkey
[b] TUBITAK, MAM, Material Institute, P.K. 21, Gebze 41470, Kocaeli, Turkey

Received 21 September 2010; received in revised form 13 November 2010; accepted 28 November 2010
Available online 21 December 2010

Abstract

In the present study, we have investigated the influence of B_2O_3 addition on structural and magnetic properties of hard magnetic $BaFe_{12}O_{19}$ foams. In the presence of B_2O_3 open-celled foams were successfully fabricated at a calcination temperature of 1300 °C. Magnetization values have been improved by 50% with B_2O_3-addition. Remanence magnetization (M_R), specific magnetization at 1.5 T (M_S) and coercive field (H_c) values were obtained to be 32.7 emu/g, 63.0 emu/g and 2100 Oe, respectively for the 0.5 wt% B_2O_3 containing foams having 30 pores/in. Foams with these magnetic properties have the potential to be used in different areas of technology as permanently magnetic materials.

PACS: 61.05.cp; 61.43.Gt; 81.05.Rm; 75.50.Ww; 81.20.Ym

Keywords: Porosity; Magnetic properties; Ferrites; Hard magnets

1. Introduction

M-type barium ferrite ($BaFe_{12}O_{19}$) has been widely used in permanent magnets, magnetic recording media and microwave devices due to its high saturation magnetization, large coercivity, good chemical stability, corrosion resistance, etc.[1–4] We have synthesized these materials in porous form by using conventional replication technique and presented the results in our previous publications.[5,6] Our studies have shown that these foam magnets are suitable for commercial use because they are permanently magnetic as well as they have light weights. Besides, their pore size lies between 0.5 mm and 1 mm. Therefore, it is possible to fill the pores by other materials having different physical properties, such as semiconducting, superconducting and polymeric materials. Thus, hybrid structures can be formed and advanced functional properties can be gained by using these materials. On the other hand, although these materials possess such functional properties, their coercive field and remanence magnetization values have been found to be low. This may be due to the application of high calcination temperatures of ∼1400 °C. Because of this, the grains, which influence the magnetic parameters, grow in an uncontrolled way. On the other hand, it was observed in our previous studies that calcination at lower temperatures produces fragile products. Besides, it has been reported that the magnetic and structural properties of barium ferrite can be improved by substituting the Fe^{3+} ions with other cations such as Co, Mn and Ru.[7–12] Boron oxide (B_2O_3) is also known to lower the melting temperature of oxide solutions.[13–17]

In the present study, our aim was to fabricate hard magnetic barium ferrite ($BaFe_{12}O_{19}$) foams of good mechanical strength and magnetic properties while keeping the calcination temperature below 1400 °C. With this purpose, we added high purity B_2O_3 powder to the initial $BaCO_3$–Fe_2O_3 mixtures in different amounts. We obtained sturdier foam magnets after calcination at 1300 °C, which is not possible without the addition of B_2O_3. In addition to this, magnetic properties have been improved significantly.

2. Experimental

Barium carbonate ($BaCO_3$) and iron oxide (Fe_2O_3) were used as the starting materials. B_2O_3 powder was added to the mix-

* Corresponding author.
E-mail addresses: ugur.topal@ume.tubitak.gov.tr (U. Topal), Halil.Bakan@mam.gov.tr (H.I. Bakan).

0955-2219/$ – see front matter © 2010 Elsevier Ltd. All rights reserved.
doi:10.1016/j.jeurceramsoc.2010.11.037

Table 1
Evolution of the lattice parameters of $BaFe_{12}O_{19}$ foams with B_2O_3 addition.

Sample (30 pores/in.)	a (Å) (±0.0008)	c (Å) (±0.0015)
Undoped	5.8932	23.2025
0.5 wt% B_2O_3	5.8926	23.2005
1.0 wt% B_2O_3	5.8921	23.2000
2.0 wt% B_2O_3	5.8927	23.2018

tures of $BaCO_3$ and Fe_2O_3 (Fe/Ba ratio was 10.5) at 0.5 wt%, 1.0 wt% and 2.0 wt%. Then the conventional replication technique was followed for the fabrication of foams.[5,6] Polyurethane sponge samples with cell sizes of 30 and 45 pores/in. were used in this study. Different pieces of the samples were calcined at different temperatures between 1000 °C and 1400 °C for 90 min. Mechanically strong foams could be achieved on samples calcined at 1300 °C and above. In order to see the influence of B_2O_3 addition on magnetic and structural properties of barium ferrite, an undoped sample was also synthesized by conventional solid state reaction method at the same conditions (1300 °C for 90 min). We must note that we did not obtain a sturdy foam structure on the undoped sample by calcination at 1300 °C.

Magnetic properties of the samples were examined at room temperature using a vibrating sample magnetometer (VSM) with a maximum applied field of 15 kOe. For microstructural analysis, samples were examined in a scanning electron microscope. X-ray diffraction analysis was performed in order to determine the phases present in the samples.

3. Results and discussion

Fig. 1 shows the XRD patterns of undoped, 0.5 wt%, 1.0 wt% and 2.0 wt% B_2O_3 added samples (calcined @ 1300 °C). It is clearly seen that $BaFe_{12}O_{19}$ is the main phase in all studied samples. The undoped sample contains large amounts of Fe_2O_3 and $BaFe_2O_4$ impurity phases. Amounts of impurity phases were determined to be ~26% and ~12% for Fe_2O_3 and $BaFe_2O_4$, respectively, from the ratios of the most intense peaks. On the other hand, impurity phases disappear with the addition of small amounts of B_2O_3 (see Fig. 1b and c). Further increase of B_2O_3 concentration to 2 wt% causes the Fe_2O_3 phase to reappear. DICVOL04 computer program was used to determine the lattice parameters of $BaFe_{12}O_{19}$ phase. As seen from Table 1, the lattice parameters tend to decrease with boron-doping, but it must be noted that such decrease seen on both a and c parameters are in the limits of uncertainty. In fact, considering the ionic radius of B^{3+} and Fe^{3+}, which is known to be 0.41 Å for B^{3+} and 0.63 Å for Fe^{3+} (i.e. not too close to each other), it is expected that lattice parameters must decrease with boron-doping if B^{3+} ions substitutes for Fe^{3+} ions. Possible crystalline modifications by B_2O_3 addition require more detailed investigations by using some refinement programs as given in Refs.[18,19] It will be topic of our future work.

Fig. 2 shows the SEM pictures of (a–d) 0.5 wt% and (e–h) 2.0 wt% B_2O_3 added foam samples fabricated using polyurethane sponge templates having cell sizes of 45 pores/in. and calcined at 1300 °C. Pore dimensions are between 300 μm and 500 μm and do not depend on the B_2O_3 concentration. As seen from Fig. 2d and h, which shows the microstructures of the struts of 0.5 wt% and 2.0 wt% B_2O_3 added foams, respectively, grains have mostly hexagonal shapes specific to the M-type barium ferrites. In addition to small-sized grains with average dimensions of ~1 μm, large grains with dimensions of up to ~10 μm are also visible in these samples. Grains are well connected to each other and almost no porosity is seen in the struts of both studied samples. On the other hand, the degree of hexagonality seems to be higher in the 0.5 wt% B_2O_3 containing sample. It follows that the 0.5 wt% B_2O_3 containing sample contains more sharp-edged grains compared to the 2.0 wt% B_2O_3 sample. The reason for this may be the higher crystallinity of the 0.5 wt% B_2O_3 sample and/or the presence of impurity phases in the 2.0 wt% B_2O_3 containing sample.

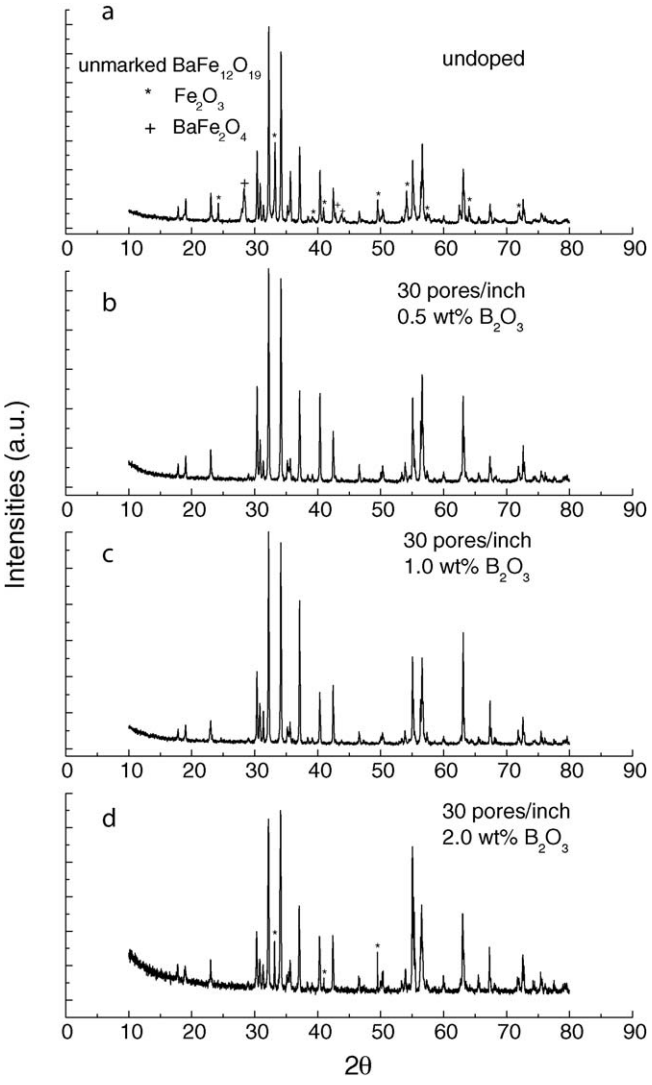

Fig. 1. The X-ray diffraction patterns of the undoped powder and B_2O_3 added foam samples.

Fig. 3 shows the M–H loops of the foam samples containing different amounts of B_2O_3. Remanence magnetization (M_R), specific magnetization at 1.5 T (M_S) and coercive field (H_c) values were extracted from these curves and given in Table 2. As

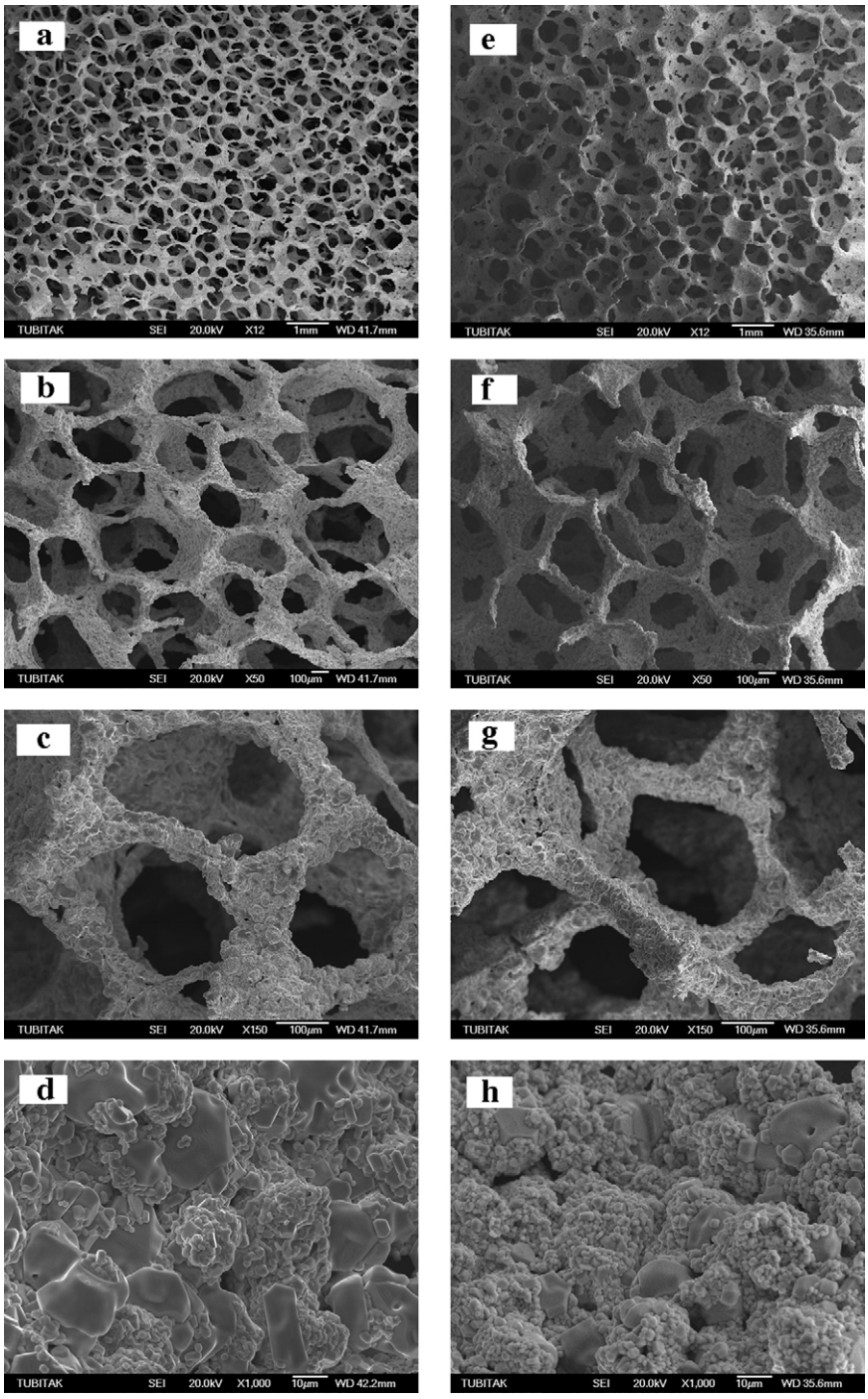

Fig. 2. SEM images of (a–d) 0.5 wt% and (e–h) 2.0 wt% B_2O_3 added foam samples (45 pores/in.) for different magnifications.

seen, B_2O_3 addition improves magnetic properties significantly. For instance, M_R and M_S (@1.5 T) values of the 0.5 wt% B_2O_3 containing material are larger than those of the undoped material by ~50% in magnitude. In fact, optimal magnetic properties are also seen at this B_2O_3 concentration, above which magnetization values start to decrease. These results are in good correlation with structural measurements. The 0.5 wt% B_2O_3 added sample has pure $BaFe_{12}O_{19}$ phase and well shaped grains. Besides, it was observed that pore sizes also contribute to the magnetization values. The M_R and M_S values of the foams having 30 pores/in. are larger than those having 45 pores/in. It must be also noted that the M_S values measured at 1.5 T is even not saturated. In order to see the real contribution of both B_2O_3 content and foam size on magnetization, saturation magnetization values (M_{S*} @ $H \rightarrow \infty$) were derived from the approach to saturation law and listed in Table 2.[20–22] As seen, saturation magnetization of 0.5 wt% B_2O_3 added sample having 30 pores/in. is 70.8 emu/g, which is very close to the theoretically estimated value of 72 emu/g.[23] Increase of pore density causes to decrease on saturation magnetization (M_{S*} = 65.7 emu/g for

Table 2
Magnetic parameters of $BaFe_{12}O_{19}$ foams.

Sample (calcination temperature)	M_R (emu/g)	M_S (emu/g) (at 1.5 T)	M_{S*} (emu/g) (at $H \rightarrow \infty$)	M_R/M_S	H_c (Oe)
Undoped (not foam) (@1300 °C)	21.5	42.6	45.6	0.505	2150
0.5 wt% B_2O_3 – 30 pores/in. (@1300 °C)	32.7	63.0	70.8	0.519	2100
1.0 wt% B_2O_3 – 30 pores/in. (@1300 °C)	23.9	60.1	64.1	0.397	1400
2.0 wt% B_2O_3 – 30 pores/in. (@1300 °C)	21.8	57.4	61.2	0.380	1100
0.5 wt% B_2O_3 – 45 pores/in. (@1300 °C)	30.5	61.8	65.7	0.493	1920
1.0 wt% B_2O_3 – 45 pores/in. (@1300 °C)	19.8	58.8	62.6	0.336	960
2.0 wt% B_2O_3 – 45 pores/in. (@1300 °C)	18.9	53.6	57.3	0.352	950
[a]Undoped – 30 pores/in. (@1400 °C)	14.3	55.1	58.2	0.259	800

[a] Data from Ref. 6.

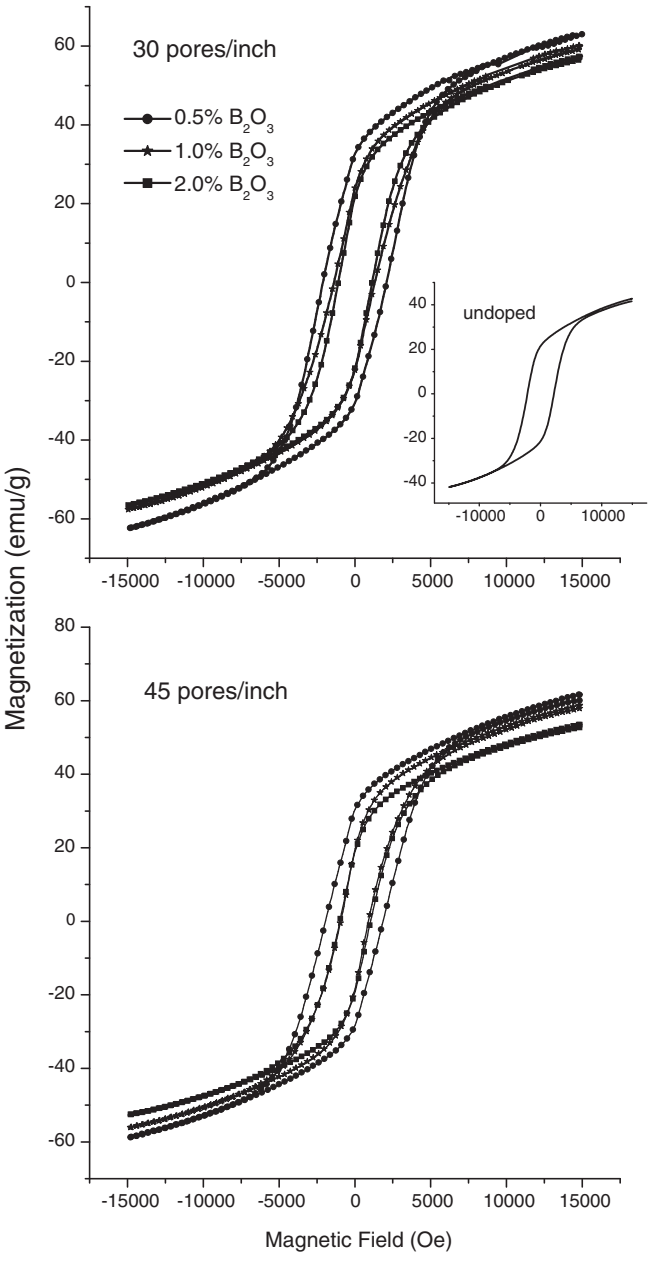

Fig. 3. The *M–H* curves as a function of pore dimensions and B_2O_3 concentration. Inset: undoped powder sample calcined at 1300 °C.

45 pores/in.). Similarly, coercive field is also much dependent on both B_2O_3 concentration and pore sizes. It decreases with increasing B_2O_3 concentration and decreasing pore size. Different factors may be responsible for the observed variations of the magnetic parameters. Effects of impurity phases, grain dimensions and the presence of porosity are some examples of these factors as discussed in the present text and in our previous studies.[6,24] The good magnetization values (M_R and M_S), and the coercive fields of foams containing 0.5 wt% B_2O_3 (which is around 2000 Oe), may make the application of these material in different areas of technology possible, for instance applications which require light weight permanent magnets.

Magnetic parameters of the undoped foams with a calcination temperature of 1400 °C and having 30 pores/inch are also given in Table 1. It is clearly seen that the addition of B_2O_3 improves all magnetic parameters significantly even if the calcination temperature is decreased to 1300 °C. The M_R, M_S (@1.5 T) and H_c values increase from 14.3 emu/g, 55.1 emu/g and 800 Oe to values as high as 32.7 emu/g, 63.0 emu/g and 2100 Oe, respectively.

4. Conclusion

The goal of the present study was to obtain hard magnetic $BaFe_{12}O_{19}$ foams by applying calcination temperatures lower than 1400 °C and to control structural properties and thus, to improve magnetic parameters of these compounds. We reached this goal by adding different amounts of B_2O_3 powder (between 0.5 wt% and 2.0 wt%) to initial $BaCO_3$ and Fe_2O_3 mixtures. Higher mechanical solidity was achieved on the foam magnets calcined at 1300 °C. Optimal magnetic properties were observed on the 0.5 wt% B_2O_3 added samples, which meet the requirements expected from a permanent magnet. Our study also reveals that magnetic parameters can be adjusted by changing the amounts of B_2O_3 content.

References

1. Wang S, Ng WK, Ding J. Preparation and characterization of Al doped longitudinal barium ferrite thin film media. *Scripta Mater* 2000;**42**:861.
2. Paul KBM. Magnetic and structural properties of Ba M-type ferrite-composite powders. *Physica B* 2007;**388**:337.
3. Yu HF, Liu PC. Effects of pH and calcination temperatures on the formation of citrate-derived hexagonal barium ferrite particles. *J Alloys Compd* 2006;**416**:222.

4. Topal U, Ozkan H, Topal KG. Improved properties of $BaFe_{12}O_{19}$ prepared by ammonium nitrate melt technique and washed in HCl. *J Alloys Compd* 2006;**422**:276.
5. Topal U, Bakan HI. Permanently magnetic $BaFe_{12}O_{19}$ foams: synthesis and characterization. *Mater Chem Phys* 2010;**123**:121.
6. Topal U, Bakan HI. Magnetic properties and remanence analysis in permanently magnetic $BaFe_{12}O_{19}$ foams. *J Eur Ceram Soc* 2010;**30**:3167.
7. Babu V, Padaikathan P. Structure and hard magnetic properties of barium hexaferrite with and without La_2O_3 prepared by ball milling. *J Magn Magn Mater* 2002;**241**:85.
8. Yang A, Chen Y, Chen Z, Vittoria C, Harris VG. Magnetic and atomic structure parameters of Sc-doped barium hexagonal ferrites. *J Appl Phys* 2008;**103**:07E511.
9. Shirtcliffe NJ, Thompson S, O'Keefe ES, Appleton S, Perry CC. Highly aluminium doped barium and strontium ferrite nanoparticles prepared by citrate auto-combustion synthesis. *Mater Res Bull* 2007;**42**:281.
10. Zhang X, Duan Y, Guan H, Liu S, Wen B. Effect of doping MnO_2 on magnetic properties for M-type barium ferrite. *J Magn Magn Mater* 2007;**311**:507.
11. Belous AG, V'yunov OI, Pashkova EV, Ivanitskii VP, Gavrilenko ON. Mössbauer study and magnetic properties of M-type barium hexaferrite doped with Co + Ti and Bi + Ti ions. *J Phys Chem B* 2006;**110**:26477.
12. Hur NH, Park JY, Dho J, Kim SJ, LeeF E.K. Magnetic and microstructural properties on Mn- and Ru-doped hexagonal barium ferrites. *IEEE Trans Magn* 2004;**40**:2790.
13. Glass HL, Stearns SF. Growth of hexagonal ferrite films by liquid phase epitaxy. *IEEE Trans Magn* 1977;**13**:1241.
14. Glass HL, Liaw JHW. Growth and characterization of LPE hexagonal ferrites. *J Appl Phys* 1978;**49**:1578.
15. Perekalina TM, Cheparin VP. Ferrimagnetism of hexagonal ferrites. *Sov Phys Solid State USSR* 1968;**9**:2524.
16. Albanese G, Deriu A. Magnetic properties of Al, Ga, Sc, In substituted barium ferrites: a comparative analysis. *Ceram Int* 1979;**5**:3.
17. Chen Y, Sakai T, Chen T, Yoon SD, Geiler AL, Vittoria C. Oriented barium hexaferrite thick films with narrow ferromagnetic resonance linewidth. *Appl Phys Lett* 2006;**88**:062516.
18. Guilmeau E, Lambert S, Chateigner D, Noudem JG, Ouladiaf B. Quantitative texture analysis of polyphased oxides by diffraction: example of Bi2223 sinter-forged ceramic and Y123 foam superconductors. *Mater Sci Eng B* 2003;**104**:107.
19. Ouhenia S, Chateigner D, Belkhir MA, Guilmeau E, Krauss C. Synthesis of calcium carbonate polymorphs in the presence of polyacrylic acid. *J Cryst Growth* 2008;**310**:2832.
20. Morales M, Chateigner D, Fruchart D. Texture and magneto-crystalline anisotropy analysis of an oriented $ErMn_4Fe_8C$ powder sample. *J Magn Magn Mater* 2003;**257**:258.
21. Li ZW, Chen L. Studies of static and high-frequency magnetic properties for M-type ferrite $BaFe_{12-2x}Co_xZr_xO_{19}$. *J Appl Phys* 2002;**92**:3902.
22. McCallum RW. Determination of the saturation magnetization, anisotropy field, mean field interaction and switching field distribution for nanocrystalline hard magnets. *J Magn Magn Mater* 2005;**292**:135.
23. Kojima H. Fundamental properties of hexagonal ferrites. In: Wohlfarth EP, editor. *Ferromagnetic Materials*, vol. 3. New York: North-Holland; 1982. p. 305–93 (chapter 3).
24. Topal U. Factors influencing the remanent properties of hard magnetic barium ferrites: impurity phases and grain sizes. *J Magn Magn Mater* 2008;**320**:331.